Mechanical Systems and Signal Processing 212 (2024) 111283

Contents lists available at ScienceDirect

Mechanical Systems and Signal Processing

journal homepage: www.elsevier.com/locate/ymssp

Rapid and restricted swing control via adaptive output feedback for 5-DOF tower crane systems

Menghua Zhang [a], Xingjian Jing [b,*], Zengcheng Zhou [c], Mingxu Sun [a]

[a] School of Electrical Engineering, University of Jinan, Jinan 250022, China
[b] Department of Mechanical Engineering, City University of Hong Kong, Hong Kong, China
[c] Department of Mechanical Engineering, The Hong Kong Polytechnic University, Hong Kong, China

ARTICLE INFO

Keywords:
Tower crane
Adaptive control
Output feedback control
Gravity compensation
Saturated control input

ABSTRACT

Crane swing & relevant vibration are critical safety and efficiency issues to be addressed in construction automation, involving various disturbance and uncertainties. This paper presents for the first time a controller designed for 5-DOF tower crane systems with no velocity signals, and its effectiveness is experimentally verified. Compared to previous controllers, the new design utilizes an adaptive output feedback control method with accurate online gravity compensation, which solves the problems of unavailability velocity, noise amplification by numerical difference, and steady state error of cable in tower crane control. Additionally, the saturated control inputs are guaranteed by employing bounded functions. The results of this study unveil that the controller proposed in this paper can simultaneously achieve accurate trolley/jib/cable positioning, rapid payload swing suppression and elimination, as well as precise payload mass estimation, and guarantee control inputs constraints. This study provides a new approach for accurate control of tower crane systems.

1. Introduction

A tower crane is an indispensable piece of equipment at a construction site, which is utilized to transport construction raw materials (payloads), including steel bars, wood, concretes, steel pipes, etc. As a type of underactuated system, where the number of control inputs less is than that of degrees of freedom, tower cranes have significant cost and flexibility advantages over the actuated system [1–3]. For tower crane systems, traditional manual manipulation has great limitations, including low work efficiency, low positioning precision, poor anti-swing performance, low safety factor, and so on [4]. Consequently, it is urgent to replace manual manipulation with safe and effective automatic control methods to improve the efficiency, security, and accuracy of the tower crane systems.

To date, control for tower crane systems has aroused the extensive attention of both researchers and engineers. In [5–7], several smooth command input shaping methods are constructed to suppress the payload swing. In [8,9], by combing the unactuated payload swing angels with the jib/trolley/cable desired trajectories, real-time trajectory planning methods with payload swing suppression performance are designed for tower crane systems under payload lowering/hoisting motion and double-pendulum effects, respectively. In [10], an optimal method to prevent collisions and reduce transportation time is proposed for multiple overlapping tower crane systems. Besides the aforementioned open-loop control method, some closed-loop control methods, including adaptive control methods [11–15], sliding mode control methods [16–19], observer-based control methods [20–22], fuzzy control methods [23,24],

* Corresponding author.
E-mail address: xingjing@cityu.edu.hk (X. Jing).

https://doi.org/10.1016/j.ymssp.2024.111283
Received 13 November 2023; Received in revised form 19 January 2024; Accepted 21 February 2024
Available online 27 February 2024

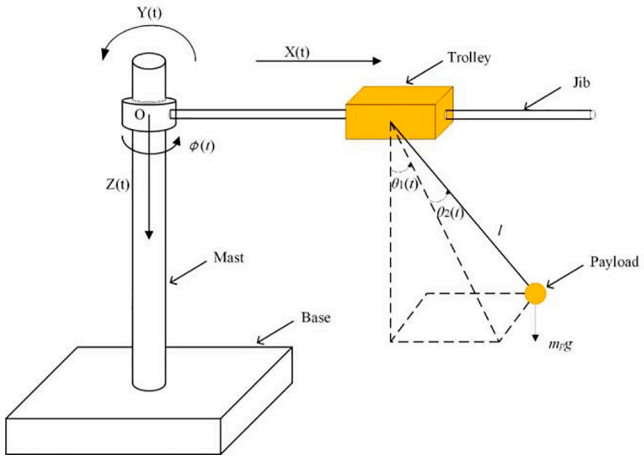

Fig. 1. Schematic illustration of tower crane systems.

end-effector motion-based method [2], neural network-based control methods [25–28], etc., are also designed for tower crane systems to improve performance. It should be pointed out that, in [11], an adaptive output feedback control method with no velocity signals is introduced for tower crane systems to realize accurate positioning and rapid payload swing suppression and elimination. To deal with the problems caused by model uncertainties and external disturbances, Trieu et al. design an adaptive fractional-order fast terminal sliding mode control method for the tower crane system with constant cable length [16]. In [21], a nonlinear disturbance observer-based feedback control method, including a robust-type term to deal with the observation error, and a switching logic function to update the unknown system parameters, is constructed for 4-DOF tower crane systems. In [2], We et al. design a robust adaptive fuzzy control method to tackle model uncertainties, parameter uncertainties, as well as external disturbances to ensure that all the system states are uniformly ultimately bounded. In our previous work [25], neural networks are employed to approximate the uncertain dynamics and nonideal control input.

Despite several control methods for tower crane systems, there are still a couple of difficulties unsolved, which are listed as follows.

1) Due to the inherent nonlinear coupling behavior, the vertical motion may trigger payload swing with a high magnitude, which makes the control issue much more complex than the constant cable length case.
2) On different occasions, tower cranes are usually utilized to transport diverse payloads, which is difficult or even unable to obtain their accurate weights, making exact gravity compensation impossible, and leading to static positioning errors.
3) Several practical application-oriented control problems, such as unavailable velocity signals, saturated control inputs, and unknown gravity compensation, remain unsolved.

For the purpose, this paper designs an amplitude-saturated output feedback control scheme without velocity signals. Additionally, to compensate for the uncertain/unknown gravity, an adaptive law is elaborately constructed. To sum up, the main contributions of this paper can be concluded as follows.

1) The designed control method can realize accurate payload positioning and rapid payload swing suppression and elimination by only available position/angle signals without additional velocity signals, avoiding velocity measurement/numerical differential operations.
2) By appropriate selection of control gains, the control inputs are theoretically limited in previously known sets, which is an important consideration in practical applications. Furthermore, the formation of the proposed control method is more straightforward than that of most existing works for 5-DOF tower crane systems and thus easier to be applied.
3) By elaborately constructing the auxiliary term of the proposed control method, accurate gravitational compensation and accurate positioning without steady errors can be guaranteed.

The outline of this paper is as follows. In Section II, the dynamic model and the problem statement are provided. Section III is devoted to the main results including the adaptive output controller design and the stability analysis. In Section IV, several experimental results are illustrated to verify the superior control performance and strong robustness of the designed control method. Section V concludes the whole paper.

2. Model and problem statement

By using Lagrange's method, the dynamic model for 5-DOF tower crane systems (given in Fig. 1) can be expressed as [29]:

Table 1
System parameters and variables.

Symbols	System parameters/variables	Units
ϕ	Jib slew angle	deg
x	Trolley displacement	m
l	Cable length	m
J	Jib rotational inertia	$kg \cdot m^2$
M_t,m_p	Jib and payload masses	kg
F_x,F_{rx}	Actuating force and friction force controlling trolley displacement	N
F_ϕ,$F_{r\phi}$	Actuating torque and friction torque controlling jib slew	$N \cdot m$
F_l,F_{rl}	Actuating force and friction force controlling cable length	N
g	Acceleration of gravity	m/s^2

$$\begin{aligned}&\left(M_t+m_p\right)\ddot{x}-m_pl\ddot{\phi}S_2+m_p\ddot{l}S_1C_2+m_pl\ddot{\theta}_1C_1C_2-m_pl\ddot{\theta}_2S_1S_2-\left(M_t+m_p\right)x\dot{\phi}^2\\&-2m_p\dot{l}\dot{\theta}_1\dot{\theta}_2C_1S_2-m_plC_2\left(S_1\left(\dot{\theta}_1^2+\dot{\theta}_2^2+\dot{\phi}^2\right)+2\dot{\phi}\dot{\theta}_2\right)-m_p\dot{l}\left(\dot{\phi}S_2-\dot{\theta}_1C_1C_2+\dot{\theta}_2S_1S_2\right)=F_x-F_{rx}\end{aligned}\tag{1}$$

$$\begin{aligned}&-m_pl\ddot{x}S_2+\left(\left(M_t+m_p\right)x^2+m_pl^2\left(S_2^2+S_1^2C_2^2\right)+2m_plxS_1C_2+J\right)\ddot{\phi}+m_px\ddot{l}S_2-m_pl^2\ddot{\theta}_1C_1S_2C_2\\&+m_pl\ddot{\theta}_2(xC_2+lS_1)+2\left(M_t+m_p\right)x\dot{x}\dot{\phi}+2m_plx\dot{\phi}\dot{\theta}_1C_1C_2+2m_pl\dot{x}\dot{\phi}S_1C_2+m_pl^2\dot{\theta}_1^2S_1S_2C_2\\&+2m_pl^2\dot{\theta}_1\dot{\theta}_2C_1S_2^2-m_plx\dot{\theta}_2\left(\dot{\theta}_2+2\dot{\phi}S_1\right)S_2+m_pl^2\dot{\phi}\dot{\theta}_1\sin(2\theta_1)S_2^2-m_pl^2\dot{\phi}\dot{\theta}_2S_1^2\sin(2\theta_2)+m_px\dot{l}S_2+m_p\dot{x}\dot{l}\dot{\theta}_2C_2=F_\phi-F_{r\phi}\end{aligned}\tag{2}$$

$$\begin{aligned}&m_p\ddot{x}S_1C_2+m_p\ddot{\phi}xS_2+m_p\ddot{l}-m_pl\dot{\theta}_1^2C_2^2-m_pl\dot{\theta}_2^2-m_p\dot{\phi}^2\left(lS_2^2+lS_1^2C_2^2-xS_1C_2\right)\\&+2m_p\dot{\phi}\dot{x}S_2+2m_pl\dot{\phi}\left(\dot{\theta}_1C_1S_2C_2-\dot{\theta}_2S_1\right)-m_pgC_1C_2=F_l-F_{rl}\end{aligned}\tag{3}$$

$$\begin{aligned}&m_pl\ddot{x}C_1C_2-m_pl^2\ddot{\phi}C_1S_2C_2+m_pl^2\ddot{\theta}_1C_2^2-m_pl(lS_1C_2+x)\dot{\phi}^2C_1C_2-m_px\dot{l}C_1C_2\\&-2m_pl^2C_2\left(\dot{\theta}_1S_2+\dot{\phi}C_1C_2\right)\dot{\theta}_2+m_pglS_1C_2+d_1\dot{\theta}_1=0\end{aligned}\tag{4}$$

$$\begin{aligned}&-m_pl\ddot{x}S_1S_2+m_pl(lS_1+xC_2)\ddot{\phi}+m_pl^2\ddot{\theta}_2+2m_pl\dot{x}\dot{\phi}C_2+m_plS_2\left(xS_1-lC_1^2C_2\right)\dot{\phi}^2\\&+2m_pl^2\dot{\phi}\dot{\theta}_1C_1C_2^2+m_pl^2\dot{\theta}_1^2S_2C_2+m_p\dot{l}\left(\dot{x}S_1S_2-\dot{\phi}xC_2\right)+m_pglC_1S_2+d_2\dot{\theta}_2=0\end{aligned}\tag{5}$$

where the system parameters and variables are illustrated in Table 1.

To facilitate the following controller design, the dynamic model described in Eqs. (1)-(5) can be expressed in the following compact form:

$$\boldsymbol{M}(\boldsymbol{q})+\boldsymbol{C}(\boldsymbol{q},\dot{\boldsymbol{q}})\dot{\boldsymbol{q}}+\boldsymbol{G}(\boldsymbol{q})=\boldsymbol{F}-\boldsymbol{F}_r\tag{6}$$

where $\boldsymbol{q}=[x\phi l\theta_1\theta_2]^T$ stands for the state vector, $\boldsymbol{F}=\left[F_xF_\phi F_l00\right]^T$ represents the control input vector, $\boldsymbol{F}_r=\left[F_{rx}F_{r\phi}F_{rl}00\right]^T$ denotes the friction vector, $\boldsymbol{M}(\boldsymbol{q})\in\mathbb{R}^{5\times5}$, $\boldsymbol{C}(\boldsymbol{q},\dot{\boldsymbol{q}})\in\mathbb{R}^{5\times5}$, and $\boldsymbol{G}(\boldsymbol{q})\in\mathbb{R}^5$ refer to the inertia matrix, the Coriolis and centrifugal matrix, and the gravity vector, respectively, the detailed expressions of which can be referred to [29].

In actual application, the length of the cable l is always positive and has a maximum value $l_{\max}$ because of limited workspace, in the sense that

$$0<l<l_{\max}\tag{7}$$

For the 5-DOF tower crane system (1)-(5), the primary aim is to drive the trolley/jib/cable to the desired positions while suppressing and eliminating the payload swing angles without using a velocity signal. In the meantime, the control inputs are kept within permitted ranges, i.e.

$$|F_x|\leqslant F_{x\max},\ |F_\phi|\leqslant F_{\phi\max},\ |F_l|\leqslant F_{l\max}\tag{8}$$

where $F_{x\max}$, $F_{\phi\max}$, $F_{l\max}$ refer to the upper bounds of F_x, F_ϕ, F_l, respectively. Moreover, for the unknown gravity m_pg, another control aim is to estimate the gravity accurately, which can be mathematically expressed as

$$\lim_{t\to\infty}\widehat{m}_pg=m_pg\tag{9}$$

where $\widehat{m}_p$ stands for the estimation of m_p.

Assumption 1. [2,3,6,9]: *The payload remains beneath the trolley, thus the payload swing is kept within the given range*:

$$-\frac{\pi}{2} < \theta_1, \theta_2 < \frac{\pi}{2} \tag{10}$$

3. Main results

In this section, the main results including both the adaptive output controller design and the stability analysis are discussed.

A. Adaptive output controller design.

To ensure accurate cable positioning without steady error, the composite function is constructed as follows:

$$\dot{p}_1 = \dot{e}_l - \lambda \tanh(p_1) \tag{11}$$

where $e_l = l - l_d$ is positioning error for the cable, l_d stands for the cable desired length, p_1 is an auxiliary function.

Additionally, to avoid utilizing velocity signals, three auxiliary functions are constructed as follows:

$$\dot{s}_1 = -k_{d1}(s_1 + k_{d1}e_x) \tag{12}$$

$$\dot{s}_2 = -k_{d2}\left(s_2 + k_{d2}e_\phi\right) \tag{13}$$

$$\dot{s}_3 = -k_{d3}(s_3 + k_{d3}e_l) \tag{14}$$

where $k_{d1}, k_{d2}, k_{d3} \in \mathbb{R}^+$ represent positive control gains, $e_x = x - x_d$ and $e_\phi = \phi - \phi_d$ are positioning errors for the trolley and the jib, respectively, x_d and ϕ_d stand for the corresponding desired positions.

Considering the system energy including the kinetic energy and the potential energy as follows:

$$V(t) = \frac{1}{2}\dot{\boldsymbol{q}}^T \boldsymbol{M}(\boldsymbol{q})\dot{\boldsymbol{q}} + m_p g l(1 - C_1 C_2) \tag{15}$$

Taking the time derivative of (15), one has

$$\begin{aligned} \dot{V}(t) &= \dot{\boldsymbol{q}}^T \boldsymbol{M}(\boldsymbol{q})\ddot{\boldsymbol{q}} + \frac{1}{2}\dot{\boldsymbol{q}}^T \dot{\boldsymbol{M}}(\boldsymbol{q})\dot{\boldsymbol{q}} + m_p g \dot{l}(1 - C_1 C_2) - m_p g l \dot{\theta}_1 S_1 C_2 - m_p g l \dot{\theta}_2 C_1 S_2 \\ &= \dot{\boldsymbol{q}}^T (\boldsymbol{U} - \boldsymbol{G}(\boldsymbol{q}) - \boldsymbol{D}(\boldsymbol{q})) + m_p g \dot{l}(1 - C_1 C_2) - m_p g l \dot{\theta}_1 S_1 C_2 - m_p g l \dot{\theta}_2 C_1 S_2 \\ &= F_\phi \dot{\phi} + F_x \dot{x} + \left(F_l + m_p g\right)\dot{l} - d_1 \dot{\theta}_1^2 - d_2 \dot{\theta}_2^2, \end{aligned} \tag{16}$$

Then, inspired by the structure of (16), the adaptive output feedback control method is constructed by utilizing (11)-(14):

$$F_x = -k_{p1}\tanh(e_x) - k_{d1}\tanh(s_1 + k_{d1}e_x) + F_{rx} \tag{17}$$

$$F_\phi = -k_{p2}\tanh\left(e_\phi\right) - k_{d2}\tanh\left(s_2 + k_{d2}e_\phi\right) + F_{r\phi} \tag{18}$$

$$F_l = -\widehat{\Delta} - k_{p3}\tanh(e_l) - k_{d3}\tanh(s_3 + k_{d3}e_l) - k_s \tanh(e_l)\left(1 - \tanh^2(e_l)\right)\tanh^2(p_1) - k_s \tanh^2(e_l)\tanh(p_1) + F_{rl} \tag{19}$$

where $k_{p1}, k_{p2}, k_{p3}, k_s \in \mathbb{R}^+$ denote positive control gains, $\widehat{\Delta}$ represents the estimate of the gravity $\Delta = m_p g$, which can be updated online by

$$\dot{\widehat{\Delta}} = k\dot{l} \tag{20}$$

where $k \in \mathbb{R}^+$ denotes a positive control gain.

Integrating (20) with respect to time, it is concluded that

$$\widehat{\Delta} = kl + \widehat{\Delta}(0) \tag{21}$$

where $\widehat{\Delta}(0)$ refers to the initial value of $\widehat{\Delta}$. Let $\widehat{\Delta}(0) \leqslant \varpi$, where $\varpi \in \mathbb{R}^+$ denotes the upper bound of $\widehat{\Delta}(0)$, from (7), we can obtain that $|\widehat{\Delta}| \leqslant k l_{\max} + \varpi$.

B. Stability analysis.

Theorem 1. *The designed control method* (17)-(19) *as well as the adaptive update law* (20), *constructed without any velocity signals, guarantee that.*

1) The actuated states x, ϕ and l asymptotically converge to their desired position/angle, in the sense that

$$\lim_{t\to\infty} x = x_d, \lim_{t\to\infty} \phi = \phi_d, \lim_{t\to\infty} l = l_d, \lim_{t\to\infty} \dot{x} = 0, \lim_{t\to\infty} \dot{\phi} = 0, \lim_{t\to\infty} \dot{l} = 0 \tag{22}$$

2) The unactuated states θ_1 and θ_2 asymptotically converge to zero, in the sense that

$$\lim_{t\to\infty}\theta_1 = 0, \lim_{t\to\infty}\theta_2 = 0, \lim_{t\to\infty}\dot{\theta}_1 = 0, \lim_{t\to\infty}\dot{\theta}_2 = 0 \tag{23}$$

3) The unknown/uncertain gravitational term $\widehat{\Delta}$ asymptotically converges to its actual value, in the sense that

$$\lim_{t\to\infty}\widehat{\Delta} = \Delta \tag{24}$$

4) The control inputs F_x, F_ϕ, and F_l are always kept within their allowable ranges, as described in (8), provided the control gains are selected to make the following inequations hold:

$$\begin{aligned} k_{p1} + k_{d1} + f_{r0x} &\leqslant F_{x\max} \\ k_{p2} + k_{d2} + f_{r0\phi} &\leqslant F_{\phi\max} \\ kl_{\max} + \varpi + k_{p3} + k_{d3} \ + \ 2k_s + f_{r0l} &\leqslant F_{l\max} \end{aligned} \tag{25}$$

where $f_{r0x}, f_{r0\phi}, f_{r0l} \in \mathbb{R}^+$ denote friction parameters, which will be defined later.

Remark 1. The following model is employed to depict the frictions [2,3,6,9]:

$$F_{rx} = f_{r0x}\tanh\left(\frac{\dot{x}}{\varepsilon_x}\right) - k_{rx}|\dot{x}|\dot{x} \tag{26}$$

$$F_{r\phi} = f_{r0\phi}\tanh\left(\frac{\dot{\phi}}{\varepsilon_\phi}\right) - k_{r\phi}\left|\dot{\phi}\right|\dot{\phi} \tag{27}$$

$$F_{rl} = f_{r0l}\tanh\left(\frac{\dot{l}}{\varepsilon_l}\right) - k_{rl}\left|\dot{l}\right|\dot{l} \tag{28}$$

where $f_{r0x}, f_{r0\phi}, f_{r0l}, \varepsilon_x, \varepsilon_\phi, \varepsilon_l, k_{rx}, k_{r\phi}, k_{rl} \in \mathbb{R}$ stand for friction-related parameters.

For short distance transferring, the trolley/jib/cable velocities are small enough so that $-k_{rx}|\dot{x}|\dot{x}$, $-k_{r\phi}\left|\dot{\phi}\right|\dot{\phi}$, $-k_{rl}\left|\dot{l}\right|\dot{l}$ can be ignored, and it can be obvious obtained that

$$|F_{rx}| \leqslant f_{r0x}, \left|F_{r\phi}\right| \leqslant f_{r0\phi}, |F_{rl}| \leqslant f_{r0l} \tag{29}$$

Proof: The following Lyapunov candidate function is constructed as follows:

$$\begin{aligned} V_{all}(t) = {} & \frac{1}{2}\dot{\boldsymbol{q}}^T\boldsymbol{M}(\boldsymbol{q})\dot{\boldsymbol{q}} + m_p g l(1 - C_1C_2) + \frac{1}{2k}\widetilde{\Delta}^2 + \ln(\cosh(e_x)) + k_{p2}\ln\left(\cosh\left(e_\phi\right)\right) + k_{p3}\ln(\cosh(e_l)) \\ & + \ln(\cosh(s_1 + k_{d1}e_x)) + \ln\left(\cosh\left(s_2 + k_{d2}e_\phi\right)\right) + \ln(\cosh(s_3 + k_{d3}e_l)) + \frac{1}{2}k_s\tanh^2(e_l)\tanh^2(p_1) \end{aligned} \tag{30}$$

Differentiating (30) with respect to time, and inserting (12)-(14), (17)-(20) into the resulting equation, it is derived that

$$\begin{aligned} \dot{V}_{all}(t) = {} & \left(F_x + k_{p1}\tanh(e_x) + k_{d1}\tanh(s_1 + k_{d1}e_x)\right)\dot{x} + \left(F_\phi + k_{p2}\tanh\left(e_\phi\right) + k_{d2}\tanh\left(s_2 + k_{d2}e_\phi\right)\right)\dot{\phi} \\ & + \left(F_l + \Delta + k_{p3}\tanh(e_l) + k_{d3}\tanh(s_3 + k_{d3}e_l) + k_s\tanh(e_l)\left(1 - \tanh^2(e_l)\right)\tanh^2(p_1) + k_s\tanh^2(e_l)\tanh(p_1)\left(1 - \tanh^2(p_1)\right)\right)\dot{l} \\ & - d_1\dot{\theta}_1^2 - d_2\dot{\theta}_2^2 - k_{d1}(s_1 + k_{d1}e_x)\tanh(s_1 + k_{d1}e_x) - k_{d2}\left(s_2 + k_{d2}e_\phi\right)\tanh\left(s_2 + k_{d2}e_\phi\right) \\ & - k_{d3}(s_3 + k_{d3}e_l)\tanh(s_3 + k_{d3}e_l) - \widetilde{\Delta}\dot{l} - k_s\tanh^2(e_l)\tanh^2(p_1)\left(1 - \tanh^2(p_1)\right) \\ = {} & - d_1\dot{\theta}_1^2 - d_2\dot{\theta}_2^2 - k_{d1}(s_1 + k_{d1}e_x)\tanh(s_1 + k_{d1}e_x) - k_{d2}\left(s_2 + k_{d2}e_\phi\right)\tanh\left(s_2 + k_{d2}e_\phi\right) \\ & - k_{d3}(s_3 + k_{d3}e_l)\tanh(s_3 + k_{d3}e_l) - k_s\tanh^2(e_l)\tanh^2(p_1)\left(1 - \tanh^2(p_1)\right) \\ \leqslant {} & 0 \end{aligned} \tag{31}$$

indicating the Lyapunov stability of the controlled system [30]. The following results can be obtained:

$$V_{all}(t) \in L_\infty \Rightarrow x, \phi, l, \theta_1, \theta_2, \dot{x}, \dot{\phi}, \dot{l}, \dot{\theta}_1, \dot{\theta}_2 \in L_\infty \tag{32}$$

Next, to prove the convergence of the states, the analysis in the invariant set Π is illustrated. Define the invariant set Π as

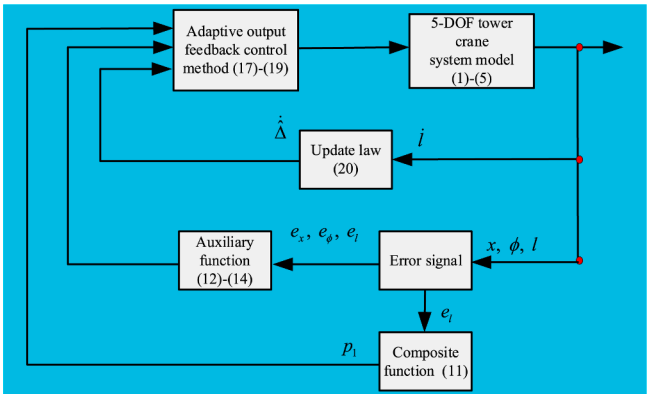

Fig. 2. Complete block diagram of the proposed control method.

$$\Pi = \left\{ \left(x, \phi, l, \theta_1, \theta_2, \dot{x}, \dot{\phi}, \dot{l}, \dot{\theta}_1, \dot{\theta}_2 \right) \middle| \dot{V}_{all}(t) = 0 \right\} \tag{33}$$

where Π_m denotes the largest invariant set in Π. Then, it can be concluded from (31) that

$$\begin{aligned} &\dot{\theta}_1 = 0, \dot{\theta}_2 = 0, \dot{s}_1 = s_1 + k_{d1} e_x = 0,\ \dot{s}_2 = s_2 + k_{d2} e_\phi = 0,\ \dot{s}_3 = s_3 + k_{d3} e_l = 0,\ e_l p_1 = 0 \\ &\Rightarrow \theta_1 = c_1, \theta_2 = c_2, \ddot{\theta}_1 = 0, \ddot{\theta}_2 = 0, s_1 = r_1, e_x = -\frac{r_1}{k_{d1}}, \\ &s_2 = r_2, e_\phi = -\frac{r_2}{k_{d2}}, s_3 = r_3, e_l = -\frac{r_3}{k_{d3}}, e_l = 0 or p_1 = 0 \\ &\Rightarrow \dot{x} = 0, \ddot{x} = 0, \dot{\phi} = 0, \ddot{\phi} = 0, \dot{l} = 0, \ddot{l} = 0 \end{aligned} \tag{34}$$

Substituting (17) and (34) into (1) becomes

$$-k_{p1} \tanh(e_x) = 0 \Rightarrow e_x = 0 \Rightarrow x = x_d \tag{35}$$

From (2), (18), and (34), the following result is obtained

$$-k_{p2} \tanh\left(e_\phi\right) = 0 \Rightarrow e_\phi = 0 \Rightarrow \phi = \phi_d \tag{36}$$

According to (4) and (34), it leads to

$$m_p g l S_1 C_2 = 0 \Rightarrow S_1 = 0 \Rightarrow \theta_1 = 0 \tag{37}$$

Similarly, combining (4) with (34) yields

$$m_p g l C_1 S_2 = 0 \Rightarrow S_2 = 0 \Rightarrow \theta_2 = 0 \tag{38}$$

From (30), if $e_l = 0$, inserting (18) and (34) into (3), it can be concluded

$$m_p g = \widehat{\Delta} \Rightarrow \Delta = \widehat{\Delta} \tag{39}$$

If $p_1 = 0 \Rightarrow \dot{p}_1 = 0$, we can obtain

$$p_1 = e_l - \lambda_3 \int \tanh(p_1) dt \Rightarrow e_l = 0 \Rightarrow \widehat{\Delta} = \Delta \tag{40}$$

By collecting the results of (39) and (40), we can get

$$l = l_d, \widehat{\Delta} = \Delta \tag{41}$$

From (25), it is easy to derive that the designed output feedback control method can guarantee the control input constraints in (8).

Then, from the results in (34)-(38), and (41), we know that Π_m contains only the equilibrium point of $\left[x \phi l \theta_1 \theta_2 \dot{x} \dot{\phi} \dot{l} \dot{\theta}_1 \dot{\theta}_2 \right]^T = [x_d \phi_d l_d 0000000]^T$. By using LaSalle's invariance theorem [30], Theorem 1 is proven.

Next, to better understand the design spirt of the designed control method, the complete block diagram is provided, and shown in Fig. 2.

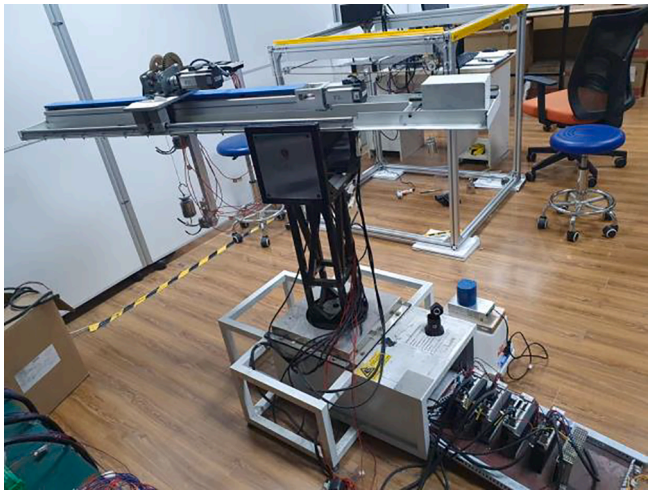

Fig. 3. Self-built tower crane testbed.

Table 2
Control gains.

Methods	Control gains
PD control method	$k_{p1}=400, k_{d1}=32, k_{p2}=250, k_{d2}=30, k_{p3}=250, k_{d3}=20$
EEMC method	$k_{p1}=300, k_{d1}=30, k_{p2}=150, k_{d2}=10, k_{p3}=250, k_{d3}=20, k_{\phi}=0.8, k_x=0.9$
Proposed control method	$k_{p1}=250, k_{d1}=32, k_{p2}=500, k_{d2}=45, k_{p3}=250, k_{d3}=20,$ $k_s=0.05, \lambda=0.5, k=0.1$

4. Experimental results and analysis

Besides the theoretical results, some hardware experiments are implemented by the self-built tower crane testbed (shown in Fig. 3) to further validate the effectiveness and robustness of the proposed controller. The motion of the jib and the trolley are actuated by two SYNTRON servo motors. The motion control board together with the control system is used to collect all state variables signals measured by the encoders and control the servo motors in real-time, simultaneously. As for the software control system, the MATLAB/Simulink RTWT (Real time Window Target) is utilized to implement the developed control method in real time. The payload is suspended from the trolley through a steel rope, whose swing motion can be conveniently captured in real time by angular encoders equipped beneath the trolley.

In Experiment 1, several system parameters are set as:

$$M_t = 3.0\text{kg}, m_p = 0.2\ \text{kg}, J = 6.8\ \text{kg}\cdot\text{m}^2, g = 9.8\text{m/s}^2$$

The friction-related parameters are given as follows:

$$f_{r0x}=2.2, \varepsilon_x=0.01, k_{rx}=-0.8, f_{r0\phi}=0.5, \varepsilon_\phi=0.01, k_{r\phi}=-0.5, f_{r0l}=0.1, \varepsilon_l=0.01, k_{rl}=-1.5$$

In addition, in Experiment 2, three cases, parameter variation, and external disturbances, are considered to test the robustness of the designed control method. Specifically, the payload mass m_p is changed from 0.2 kg to 0.5 kg. Moreover, extraneous disturbances are artificially introduced. In Experiments 1 and 2, the initial and desired trolley/jib/cable positions/angles/lengths are set as

$$x(0)=0\ \text{m}, \phi(0)=0\ \text{deg},\ l(0)=0.3\ \text{m}, x_d=0.3\ \text{m}, \phi_d=30\ \text{deg},\ l_d=0.6\ \text{m}$$

The control gains of the designed control method in Experiments 1 and 2 are tuned as given in Table 2.

4.1. Experiment 1: effectiveness validation

For the sake of testing the satisfactory control performance of the designed adaptive output feedback control method, the traditional PD control method and the end-effector motion-based (EEM)control method are employed as comparative methods. The control gains of these control methods are illustrated in Table II. The experimental results are shown in Fig. 4. Apparently, in the case of similar rising time (all within 4 s), the designed control method could yield better results than these two comparative methods. Exactly speaking, the presented control method suppresses the payload swing angles within smaller ranges ($\theta_{1\max}=1.1$ deg, $\theta_{2\max}=0.9$ deg, as well as almost no residual swing angles). In addition, the proposed control method considerably reduces the payload swing suppression and elimination time consumption (which is defined as time when $|\theta_1|, |\theta_2| \leqslant 0.2$ deg) up to 50 % in comparison with other

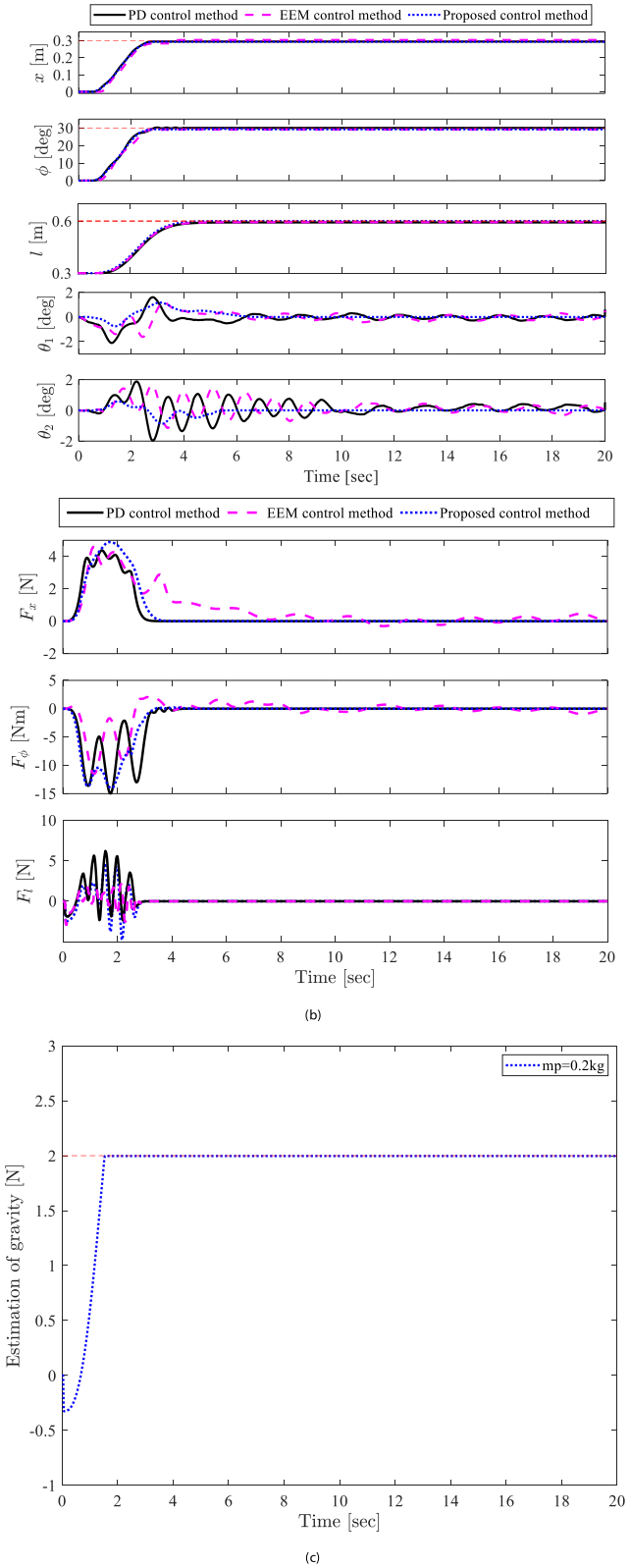

Fig. 4. Experiment 1: Results of PD control method, EEM control method, and proposed control method.

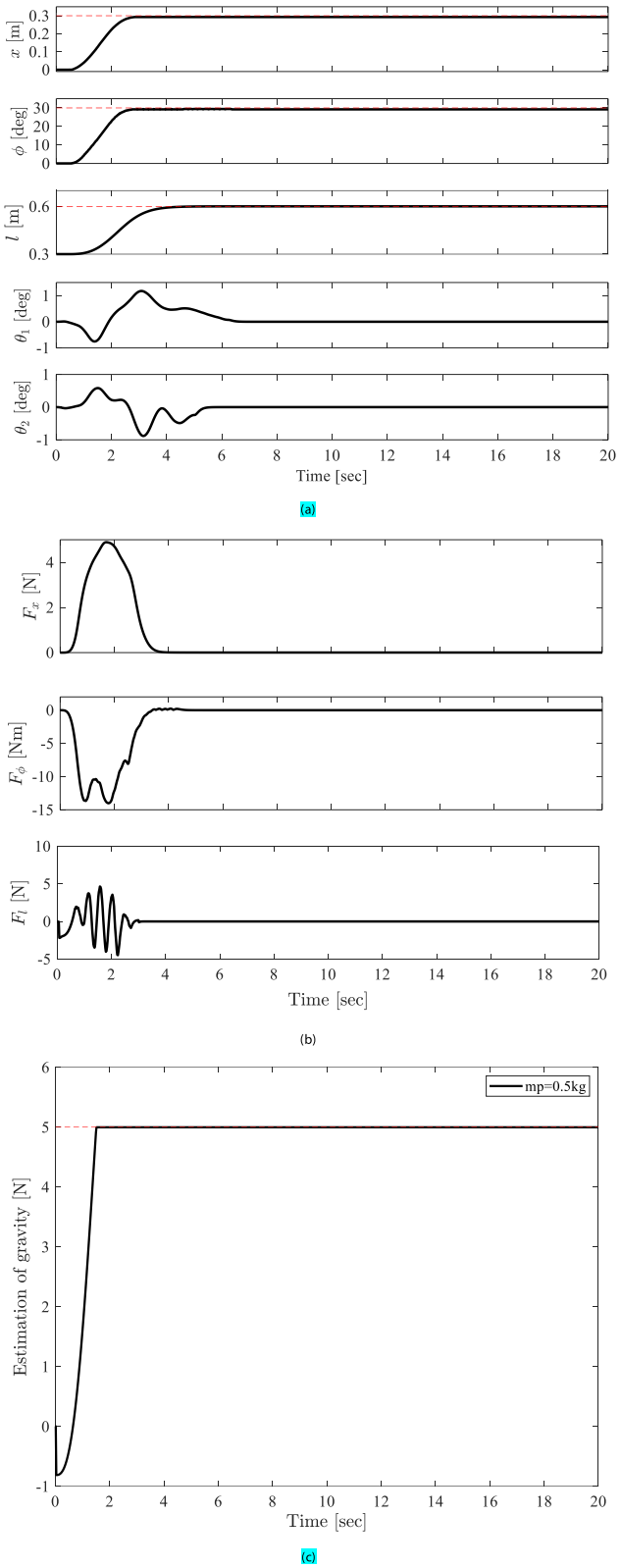

Fig. 5. Experiment 2: Results for the proposed control method with respect to Case 1.

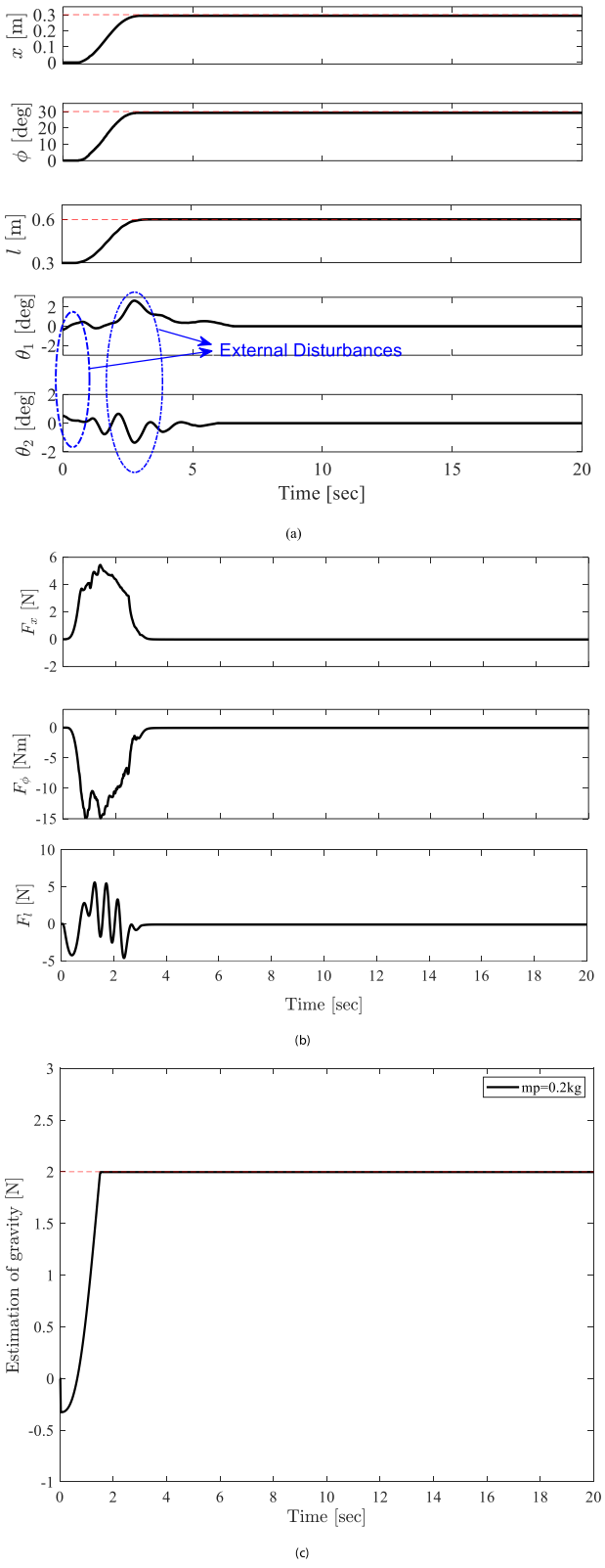

Fig. 6. Experiment 2: Results for the proposed control method with respect to Case 2.

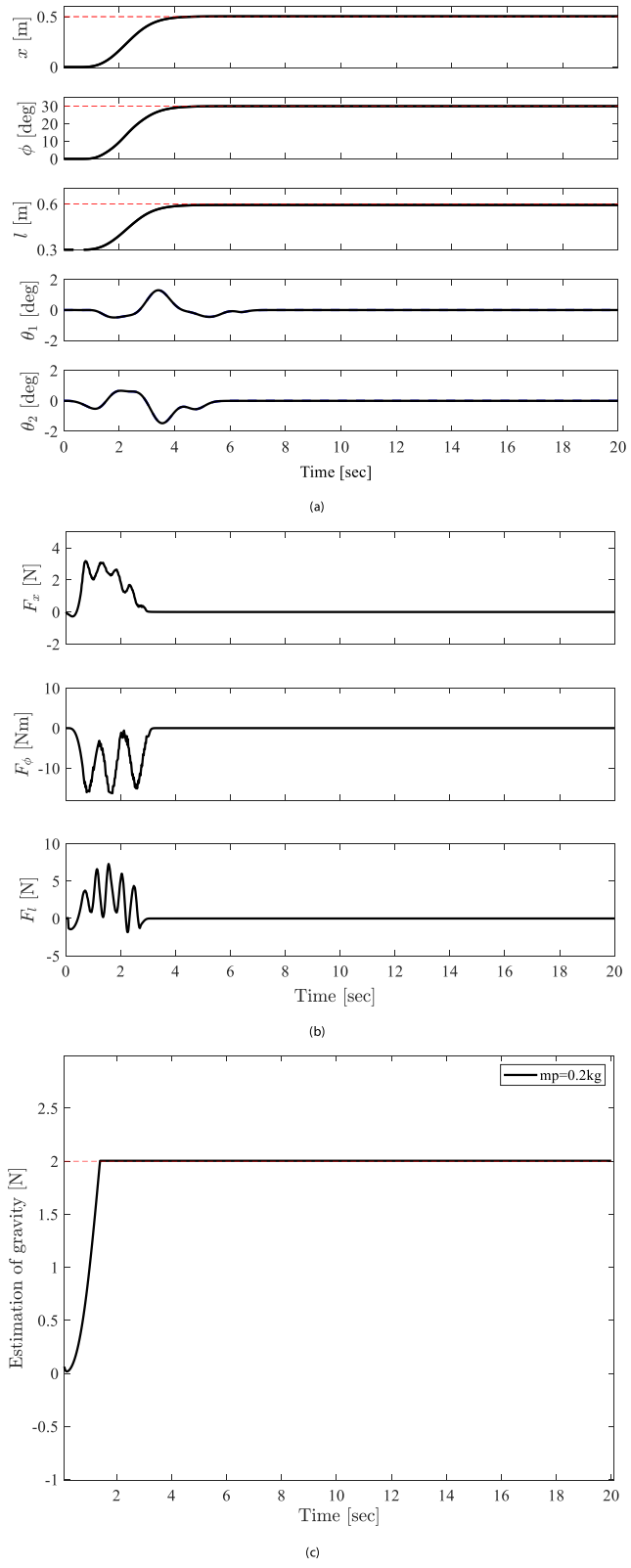

Fig. 7. Experiment 2: Results for the proposed control method with respect to Case 3.

control methods. In addition, the designed control method estimates the gravity accurately, and hence could achieve satisfactory positioning results without positioning errors.

4.2. Experiment 2: robustness validation

Case 1. Parameter variation. The payload mass m_p is changed to 0.5 kg. As shown in Fig. 5, even if the actual value of the payload mass is quite different from its nominal value, the constructed adaptive output control method could still have superior control performance including positioning and anti-swing suppression, indicating it admits strong robustness with respect to uncertain payload mass/gravity.

Case 2. External disturbances. Besides robustness regarding system parameter variations, the designed control method also presents strong anti-interference capability. More precisely, to better emulate external disturbances, we drag the payload artificially at about 0 s and 3 s. From Fig. 6, we can observe that the 5-DOF tower crane system controlled by the proposed adaptive output control method presents strong robustness against these external disturbances; and the trolley/jib/cable could reach their desired position/angle/length with very few positioning errors.

Case 3. Different trolley positions. To verify the control performance of the designed control method with respect to different traveling disturbances while the control gains remain the same as those in Experiment 1. We set the trolley desired position as $x_d = 0.5$ m. From Fig. 7, it is observed that the proposed control method can push the trolley to reach the desired positions accurately as well as suppress and eliminate the payload swing quickly.

5. Conclusion

An adaptive output feedback control method considering input constraints, uncertain/unknown payload mass, and unavailable velocity signals is proposed for 5-DOF tower crane systems. The resulting control method can guarantee precise trolley/jib/cable transferring as well as rapid payload swing suppression and elimination. Besides its implementation simplicity, the significant advantage of the designed control method is that it can guarantee few static positioning errors using only position signals, in spite of the uncertainties and input constraints. The robustness to unknown payload gravity is also analyzed. Specifically, for the proposed controller, a composite function is constructed to guarantee precise cable positioning, several auxiliary functions are employed to replace the velocities, an adaptive scheme is designed to identify uncertain/unknown payload mass, and hyperbolic tangent functions are introduced to satisfy control input constraints. The Lyapunov-based analysis is carried out to prove the control performance of the designed control method. Also, experiments are illustrated to confirm its satisfactory performance, where the payload mass, as well as the velocity signals, are not required to be measured. This could be more interesting in practical applications. Future work will focus on actuator fault-tolerant control investigation.

CRediT authorship contribution statement

Menghua Zhang: Conceptualization, Funding acquisition, Methodology. **Xingjian Jing:** Supervision. **Zengcheng Zhou:** Software. **Mingxu Sun:** Writing – review & editing.

Declaration of competing interest

The authors declare the following financial interests/personal relationships which may be considered as potential competing interests: Menghua Zhang reports financial support was provided by National Natural Science Foundation of China. Menghua Zhang reports financial support was provided by the Outstanding Youth Foundation of Shandong Province. Xingjian Jing reports financial support was provided by the Startup Fund of City University of Hong Kong. Menghua Zhang reports financial support was provided by the Key R&D Project of Shandong Province. If there are other authors, they declare that they have no known competing financial interests or personal relationships that could have appeared to influence the work reported in this paper.

Data availability

No data was used for the research described in the article.

Acknowledgements

This work was supported in part by the National Natural Science Foundation of China under Grant No. 62273163, the Taishan Scholar Foundation of Shandong Province, the Outstanding Youth Foundation of Shandong Province under Grant No. ZR2023YQ056, the Startup Fund of City University of Hong Kong under Grant No. 9380140, the NSFC/RGC project (CityU 11202323), the general research fund of HK RGC (N_CityU114/23), and the Key R&D Project of Shandong Province under Grant No. 2022CXGC010503.

References

[1] F. Rauscher, O. Sawodny, Modeling and control of tower cranes with elastic structure, IEEE Trans. Control Syst. Technol. 29 (1) (Jan. 2021) 64–79.

[2] N. Sun, Y. Fang, New energy analytical results for the regulation of underactuated overhead cranes: an end-effector motion-based approach, IEEE Trans. Ind. Electron. 59 (12) (Dec. 2012) 4723–4734.
[3] M. Zhang, X. Jing, Model free saturated PD-SMC method for 4-DOF tower crane systems, IEEE Trans. Ind. Electron. 69 (10) (Oct. 2022) 10270–10280.
[4] J. Huang, W. Wang, J. Zhou, Adaptive control design for underactuated cranes with guaranteed transient performance: theoretical design and experimental verification, IEEE Trans. Ind. Electron. 69 (3) (Mar. 2022) 2822–2832.
[5] S.M.F.U. Rehman, Z. Mohamed, A.R. Husain, H.I. Jaafar, M.H. Shaheed, M.A. Abbasi, Input shaping with an adaptive scheme for swing control of an underactuated tower crane under payload hoisting and mass variations, Mech. Syst. Sig. Process. 175 (Aug. 2022) 109106.
[6] T. Yang, N. Sun, H. Chen, Y. Fang, Swing suppression and accurate positioning control for underactuated offshore crane systems suffering from disturbances, IEEE/CAA J. Autom. Sin. 7 (3) (May 2020) 892–900.
[7] A. Al-Fadhli and E. Khorshid, "Payload oscillation control of tower crane using smooth command input," *Journal of Vibration and Control*, in press, DOI: 10.1177/10775463211054640.
[8] Z. Tian, L. Yu, H. Ouyang, G. Zhang, Swing suppression control in tower cranes with time-varying rope length using real-time modified trajectory planning, Autom. Constr. 132 (Sep. 2021) 103954.
[9] H. Ouyang, Z. Tian, L. Yu, G. Zhang, Motion planning approach for payload swing reduction in tower cranes with double-pendulum effect, J. Franklin Inst.-Eng. Appl. Math. 357 (13) (2020) 8299–8320.
[10] C. Huang, W. Li, W. Lu, F. Xue, M. Liu, Z. Liu, Optimization of multiple-crane service schedules in overlapping areas through consideration of transportation efficiency and operation safety, Autom. Constr. 127 (Apr. 2021) 103716.
[11] Y. Wu, N. Sun, H. Chen, Y. Fang, Adaptive output feedback control for 5-DOF varying-cable-length tower cranes with cargo mass estimation, IEEE Trans. Ind. Inf. 17 (4) (2021) 2453–2464.
[12] J. Huang, W. Wang, J. Zhou, Adaptive control design for underactuated cranes with guaranteed transient performance: theoretical and design and experimental verification, IEEE Trans. Ind. Electron. 69 (3) (2022) 2822–2832.
[13] J. Kim, D. Lee, B. Kiss, D. Kim, An adaptive unscented Kalman filter with selective scaling (AUKF-SS) for overhead cranes, IEEE Trans. Ind. Electron. 68 (7) (2021) 6131–6140.
[14] P. Shen, J. Schatz, R.J. Caverly, Passivity-based adaptive trajectory control of an underactuated 3-DOF overhead crane, Control Eng. Pract. 112 (2021) 104834.
[15] M. Li, H. Chen, and R. Zhang, "An input dead zones considered adaptive fuzzy control approach for double pendulum cranes with variable rope lengths," *IEEE/ASME Transactions on Mechatronics*, in press, DOI: 10.1109/TMECH.2021.3137818.
[16] P.V. Trieu, H.M. Cuong, H.Q. Dong, N.H. Tuan, L.A. Tuan, Adaptive fractional-order fast terminal sliding model with fault-tolerant control for underactuated mechanical systems: application to tower cranes, Autom. Constr. 123 (2021) 103533.
[17] H.M. Cuong, H.Q. Dong, P.V. Trieu, L.A. Tuan, Adaptive fractional-order terminal sliding mode control of rubber-tired gantry cranes with uncertainties and unknown disturbances, Mech. Syst. Sig. Process. 154 (2021) 107601.
[18] L.A. Tuan, Neural observer and adaptive fractional-order backstepping fast-terminal sliding-mode control of RTG cranes, IEEE Trans. Ind. Electron. 68 (1) (2021) 434–442.
[19] X. Gu, H. Zhou, M. Hong, S. Ye, and Y. Guo, "Adaptive hierarchical sliding mode controller for tower cranes based on finite time disturbance observer," *International Journal of Adaptive Control and Signal Processing*, in press, DOI: 10.1002/acs.3458.
[20] H. Ren, Z. Cheng, J. Qin, and renquan lu, "deception attacks on event-triggered distributed consensus estimation for nonlinear systems", Automatica 154 (2023) 111100.
[21] Y. Qian, Y. Fang, Switching logic-based nonlinear feedback control of offshore ship-mounted tower cranes: a disturbance observer-based approach, IEEE Trans. Autom. Sci. Eng. 16 (3) (2019) 1125–1136.
[22] J.H. Ye, J. Huang, Analytical analysis and oscillation control of payload twisting dynamics in a tower crane carrying a slender payload, Mech. Syst. Sig. Process. 158 (2021) 107763.
[23] L. Dong, H. Zhang, K. Yang, D. Zhou, J. Shi, J. Ma, Crowd counting by using top-k relations: A mixed ground-truth CNN framework, IEEE Trans. Consum. Electron. 68 (3) (2022) 307–316.
[24] R.C. Roman, R.E. Precup, E.M. Petriu, Hybrid data-driven fuzzy active disturbance rejection control for tower crane systems, Eur. J. Control. 58 (2021) 372–387.
[25] M. Zhang, X. Jing, Adaptive neural network tracking control for double-pendulum tower crane systems with nonideal inputs, IEEE Trans. Sys. Man Cybernetics: Sys. 52 (4) (2022) 2514–2530.
[26] Y. Qian, D. Hu, Y. Chen, Y. Fang, Y. Hu, Adaptive neural network-based tracking control of underactuated offshore ship-to-ship crane systems subject to unknown wave motions disturbances, IEEE Trans. Sys. Man Cybernetics: Sys. 52 (6) (2022) 3626–3637.
[27] T. Yang, N. Sun, and Y, Fang, "Neuroadaptive control for complicated underactuated systems with simultaneous output and velocity constraints exerted on both actuated and unactuated states," IEEE Transactions on Neural Networks and Learning Systems, in press, DOI: 10.1109/TNNLS.2021.3115960.
[28] T. Yang, H. Chen, N. Sun, Y. Fang, "Adaptive neural network output feedback control of uncertain underactuated systems with actuated and unactuated state constraints," IEEE Transactions on Systems, Man, Cybernetics: Systems, vol. 52, no. 11, pp. 7027-7043.
[29] M. Zhang, Y. Zhang, B. Ji, C. Ma, X. Cheng, Adaptive sway reduction for tower crane systems with varying cable lengths, Autom. Constr. 119 (Nov. 2020) 103342.
[30] H.K. Khalil, Nonlinear systems, 3rd ed., Prentice-Hall, Englewood Cliffs, NJ, 2002.